Solid Earth Discuss., 5, 2419–2448, 2013
www.solid-earth-discuss.net/5/2419/2013/
doi:10.5194/sed-5-2419-2013

Solid Earth
Discussions
Open Access

Optimal locations of sea-level indicators in glacial isostatic adjustment investigations

H. Steffen[1], P. Wu[2,*], and H. Wang[3]

[1]Lantmäteriet, Lantmäterigatan 2c, 80182 Gävle, Sweden
[2]Department of Geoscience, University of Calgary, 2500 University Drive NW, Calgary, AB, T2N 1N4, Canada
[3]State Key Laboratory of Geodesy and Earth's Dynamics, Institute of Geodesy and Geophysics, Chinese Academy of Sciences, Wuhan 430077, China
[*]now at: The University of Hong Kong, Hong Kong, China

Received: 19 November 2013 – Accepted: 29 November 2013 – Published: 18 December 2013

Correspondence to: H. Steffen (holger-soren.steffen@lm.se)

Published by Copernicus Publications on behalf of the European Geosciences Union.

Abstract

Fréchet (sensitivity) kernels are an important tool in glacial isostatic adjustment (GIA) investigations to understand lithospheric thickness, mantle viscosity and ice-load model variations. These parameters influence the interpretation of geologic, geophysical and geodetic data, which contribute to our understanding of global change. Recently, sensitivity kernels have been extended to laterally heterogeneous Earth models using the finite-element formulation, which enabled detailed studies on the sensitivity of the different geodetic observations of GIA such as GPS and terrestrial and space gravimetry.

In this study, we discuss global sensitivities of relative sea-level (RSL) data of the last 18 000 yr. This also includes indicative RSL-like data (e.g. lake levels) on the continents far off the coasts. We present detailed sensitivity maps for four parameters important in GIA investigations (ice-load history, lithospheric thickness, background viscosity, lateral viscosity variations) for up to 9 dedicated times. Assuming an accuracy of 2 m of RSL data of all ages, we highlight areas around the world where, if the environmental conditions allowed its deposition and survival until today, RSL data of at least this accuracy may help to quantify the GIA modelling parameters above.

The sensitivity to ice-load history variations is the dominating pattern covering in times of 14 ka BP and older almost the whole world. Lithospheric thickness variations are mainly only possible to be determined in certain high-latitude areas around the large former and current ice sheets. Background viscosity as well as lateral viscosity variations can be traced at most coast and shelf areas around the world, especially when dated to be older than 10 ka BP. The latter three are almost everywhere overlapped by the ice-load history pattern. In general we find that the more recent the data are, the smaller is the area of possible RSL locations which could provide enough information on the four GIA modelling parameters. But, we also note that when the accuracy of RSL data can be improved, e.g. from 2 m to 1 m, these areas become larger allowing better inference of background viscosity and lateral heterogeneity. Although the patterns depend on the chosen models and error limit, our results are indicative

enough to outline areas where one should look for helpful RSL data of a certain time period.

1 Introduction

Glacial isostatic adjustment (GIA) describes the response of the Earth to glacial loading and unloading processes. It includes changes in the Earth's deformation, gravity due to redistribution of mass, moment of inertia and state of stress. Hence, investigations to GIA address different fields giving among other things insight into ice-load dynamics and Earth rheology. For the latter, foci are mainly set with GIA models on lithospheric thickness and mantle viscosities as well as their lateral variation in the Earth, respectively.

For an accurate determination of model parameters such as ice-load history, lithospheric thickness, radial and lateral variation of mantle viscosities, many geologic, geophysical and geodetic observations are used to constrain GIA models or identify the best-fitting one by comparing the observation to model predictions (see e.g. Steffen and Wu, 2011, for an overview). Nowadays, the most commonly used observations are GPS measurements, which provide a highly accurate current velocity/deformation field, and gravimetric observations based on terrestrial (absolute and relative gravimetry) and space techniques, which show the deviation from equilibrium and ongoing mass redistributions (Wu et al., 2013). It should be noted that both GPS land-uplift rate and gravity rate-of-change data only give the rate-of-change today, which is more than 8000 yr after the end of deglaciation. On the other hand, relative sea-level (RSL) data record the deformation occurred in the past (Wu et al., 2013), especially in the last about 20 000 yr since the times of the Last Glacial Maximum (LGM).

The determination of ice-load history, lithospheric thickness and mantle viscosity highly depends on the quality and thus accuracy of the used data. Geodetic observations achieve sufficient accuracy for the detection of the GIA signal after a few years, i.e. about 5 yr, of observation (Wu et al., 2010; Steffen et al., 2012). The longer the time span is, the better is the accuracy. Knowledge of these facts enabled Wu et al. (2010) and Steffen et al. (2012) to investigate the sensitivity of GPS and gravity observations, respectively, to four prominent GIA modelling parameters: ice-load history, lateral lithospheric thickness variation, background viscosity, and lateral viscosity variation. The major goal of the two studies was to identify optimal locations for these geodetic observations as economic, logistic and ecological reasons limit the capabilities to sufficiently cover the (whole) Earth with stations (Steffen et al., 2012). An optimal location is here defined by where sensitivity lies above the current accuracy of a selected geodetic observation (Wu et al., 2010).

Wu et al. (2010) studied the optimal locations for GPS measurements in North America and Fennoscandia, both areas with prominent GIA signals and already existing GPS networks. They clearly identified the region west of Hudson Bay until the Rocky Mountains as a major gap in the North American permanent GPS network. In contrast, the network in northern Europe is almost adequate (Wu et al., 2010). Ice-load history appeared to be the best detectable parameter.

The study by Steffen et al. (2012) focused on optimal locations of terrestrial (absolute) gravity measurements in North America and northern Europe and also analyzed the sensitivity of the Gravity Recovery and Climate Experiment (GRACE) twin-satellite mission there to the four parameters. Both terrestrial measurements and GRACE observations sense the four parameters as their sensitivity is higher than the currently determined trend errors, with ice-load history being again the best detectable parameter (Steffen et al., 2012). The authors also suggested more absolute gravity stations in northwestern and Arctic Canada and a comprehensive data combination of all absolute gravity measurements in northern Europe.

This study adds RSL data now to the search for optimal locations of GIA observations to help constrain parameters used in GIA modelling. RSL data have since the beginning of GIA research been an important dataset in the understanding and modelling of the GIA process (Steffen and Wu, 2011). Still, they help in constraining ancient ice history (Peltier, 2004; Horton et al., 2009; Engelhart et al., 2011), quantifying the timing of drainage of glacial lakes (Törnqvist and Hijma, 2012) or apparent uplift of the coast since the last interglacial 125 000 yr ago (Pedoja et al., 2011).

The issue and analysis here is different to the former studies with geodetic data in at least three ways. First, GPS and gravity measurements represent recent measurements that determine the GIA signal today. The signal is small, i.e. about 1 $\mathrm{cm\,a^{-1}}$ vertical change and about 2 $\mathrm{\mu Gal\,a^{-1}}$ gravity change, while RSL data may show a complete deformation curve over several thousands of years with occasionally several hundreds of meters. Thus, a geodetic signal can be considered as a snapshot of the time-delayed visco-elastic part of GIA, and the observations are "only" three-dimensional when compared to the four-dimensional (space and time) signal visible in RSL data. Hence, we compare something recent (GPS, gravity) with something from the past (RSL) (Wu et al., 2013).

Second, we turn to sea-level indicators that have to be deposited under certain conditions to survive until today. While GPS and terrestrial gravity measurements are limited due to economic and/or logistic reasons, RSL data can potentially be found in all oceans and coastal areas. Also, RSL-like data such as lake levels can be found far off the coast, e.g. in Sweden (Lambeck et al., 1998a). However, there are different limitations depending on the sea-level indicator itself, the environment of its deposition, processes acting at the sample or in the area since its deposition, and many more. We can only use what has survived the last few thousand years as we cannot go back in time and protect them. Thus, the difference to the former sensitivity studies discussed above is that we cannot advice where to place instruments for adequate measurements, but we can outline, however not guarantee, where RSL data with sufficient information could be found. In addition, we can illustrate the sensitivity of RSL data on a global scale rather than the dedicated regions we had to use for geodetic observations.

Third, the sensitivity of RSL data varies with time. The same naturally holds for the sensitivity of geodetic observations as well, however, as aforementioned, geodetic measurements are only snapshots of today. Thus, we have to analyze different times when RSL data were likely deposited, also depending on the accuracy to be achieved with current dating methods.

In view of the remarks above, we address the following questions in this paper:

- Where should RSL data be located to help constrain ice-load history models, lateral lithospheric thickness variations, background viscosity and lateral viscosity variations used in GIA modelling?
- At which times are RSL data at a certain location sensitive to one of the parameters?
- How accurate should they be?
- Where should new and helpful data be searched?

In the next section, we discuss RSL data, their errors and possible deposition times. This is followed by Sect. 3 which gives an introduction of the models used. Sections 4 and 5 present and discuss the results, respectively. Based on the discussion of RSL data in Sect. 2, we provide complete maps of RSL data sensitivities for 9 different times in the past. Finally, the conclusion is given in Sect. 6.

2 Relative sea-level data

Relative sea levels or paleo-strandlines document the crustal response of the Earth due to glaciation and subsequent water mass redistribution between the oceans and ice sheets. The sea level at a certain time and location can be dated by shells, corals, wood, whale bones or pollen (van de Plassche, 1986). Their great benefit is that they cover a long time period of deformation, occasionally dating back to several thousand years (Steffen and Wu, 2011). They are mostly dated by ^{14}C method and thus need to be calibrated for use in GIA modelling.

Sea-level indicators can be found in coastal and shelf areas all around the world. However, their quality and age vary from location to location as many processes such

SED
5, 2419–2448, 2013

as changes in tidal range, storms, local tectonics, and compaction (see e.g. Vink et al., 2007) influence their deposition and preservation. Also, the last ice sheets have destroyed evidence of previous shorelines leading to lack of data from before 20 ka BP in formerly glaciated areas (Steffen and Wu, 2011). In northern Europe, for example, one can find about 4000 dated sea-level indicators, with most data going back to about 15 ka BP (Steffen and Wu, 2011). However, not all are publicly available (see Lambeck et al., 2010). All over the world, several thousand data have been collected so far (Klemann and Wolf, 2006), but new data emerge occasionally and are added to existing databases.

Figure 1 shows the distribution of RSL data in our database in northern Europe and North America. It can be seen that older data are found outside the former glaciation. The closer the data are located to the last remnants of the ice sheets, the younger they are. The flooding of the southern North Sea is also mirrored in older data in the sea and younger data near the coast.

Now, each sample of a database has an associated error or uncertainty in height *and* time. This is different to GPS and gravity measurements, which are usually provided with an error in velocity or gravity-rate-of-change, respectively. Thus, when investigating the observational error of RSL data one has to consider two errors. However, the time error of RSL data is often converted into an additional height error (Lambeck et al., 1998b) to ease a misfit calculation. The height error then includes the effect $|\mathrm{d}h/\mathrm{d}t|_t \sigma_t$ (Lambeck et al., 1998b), with $|\mathrm{d}h/\mathrm{d}t|_t$ the rate of sea-level change at time t and σ_t the age error. The rate of sea-level change is usually taken from a rebound model, which is determined as part of an iterative solution in ice-model developments (Lambeck et al., 2010). Hence, the height error becomes larger while the time error is set to zero. An excellent discussion of error sources in RSL data can be found in Lambeck et al. (1998b).

As an example, we analyze our available data sets for North America and northern Europe (including the British Isles) for their errors. The aim of this exercise is to find a reliable average error that can be applied in this investigation. For 11 time periods that

SED
5, 2419–2448, 2013

we analyze in total (see Sect. 4), we group our data accordingly in subsets of 1000 or 2000 yr duration. Figure 2 shows the average and maximum RSL data errors in North America and northern Europe. About 3700 data samples were analyzed, which cover a large range in time and space. We thus consider our determined average value below to be significant for all possibly available RSL data.

Groups of younger samples contain many hundreds of samples, while groups with older samples, e.g. of 14 ka BP and older, envelope only a few. The maximum error becomes larger the older the subset is, peaking at 10 (North America) and 12 ka BP (northern Europe), and then becoming much smaller (especially for North America). However, the number of older data is, as outlined above, much smaller than the number of younger data, therefore this error range is biased by the number of samples in each time span. One should also consider that the database partly contains samples analyzed a few decades ago when dating methods were not as sophisticated as today, and thus such samples may have larger errors. These errors may increase the average error of a time span. But, we use our database as a typical example with a sufficiently high number of samples allowing a robust analysis. It is beyound the aims of this study to evaluate each of the 3700 data samples how and when it was dated.

North American data overall support an average error value of 2 m during all time subsets (thin solid black line in Fig. 2). Fennoscandian data show a higher average than 2 m for 10 ka BP and older. However, we hope that more newly determined data to be added to these time subsets will lower the average. For example, new data for the southern North Sea show mainly errors of much less than a meter (Vink et al., 2007). Thus, we set 2 m as limit in our study, but we also test in two examples how a better error of 1 m as well as an extrem value of 8 m (e.g. the average error of Fennoscandian data at 12 ka BP) affect our results.

3 Modelling

The models and approach used are taken from Wu et al. (2010) and Steffen et al. (2012). In summary, we use a reference model with 115 km lithospheric thickness as well as 6×10^{20} Pa s, 3×10^{21} Pa s and 6×10^{21} Pa s as background viscosity in the upper, shallower lower and deep lower mantle, respectively. The ice-load history is taken from model Ice-4G (Peltier, 1994). Both are employed in a non-rotating, spherical, self-gravitating, Maxwell visco-elastic Finite Element earth model which includes material compressibility and self-gravitating oceans. We then vary one of these parameters in the model to test its sensitivity on a global scale for RSL data. This is different to the former papers as they focused on North America and Fennoscandia only. The reference model and an overview of the varied parameters can be found in Table 1.

For the sensitivity to the ice model, we compared the response between Ice-4G and Ice-5G (Peltier, 2004) globally (which differ not only in the Northern Hemisphere but also in Antarctica). This is slightly different to the former studies as we tested the sensitivity of Ice-4G to the ANU-Ice ice model by Lambeck et al. (1998b) in Fennoscandia. For the other three parameters we apply the same changes as in Steffen et al. (2012). Therefore, for the lateral heterogeneous lithospheric thickness a model by Wu et al. (2005) is used. The background viscosity is changed to 7×10^{20} Pa s in the upper mantle and 10^{22} Pa s throughout the lower mantle. Thus, we modify a VM2-like model (Wu et al., 2013) with a slight gradual viscosity change from the upper to the lower mantle to one with a higher viscosity contrast with depth. The lateral heterogeneous mantle viscosity is implemented from model RF3S20 by Wang et al. (2008).

As in former studies, we caution that the model parameters used represent typical cases only. We do not provide definitive sensitivity results. This is not anticipated as we apply selected models for ice-load history, lateral lithospheric thickness and viscosity, and there exists a broad variety of models and opinions for each parameter. There is, for example, still no consensus about how viscosity increases with depth in the mantle (Steffen and Wu, 2011; Wu et al., 2013). Hence, it is rather our goal to give a feel of what sensitivity one may expect in general, and also, where we can expect or look for RSL data that may help solve problems still under debate.

4 Results

We determine the sensitivity kernels for 11 different times from 18 ka BP until 2 ka BP. Time steps are 2000 yr, and we additionally calculate the sensitivity for 9 and 7 ka BP as the large continental ice sheets completely vanish during the period from 10 ka BP until 6 ka BP. As we are interested in four different parameters, this would result in a large number of 44 figures or subplots. Therefore, we show two distinct examples only. The first is an overview of 6 sensitivity patterns for a changed ice-load history at 18, 16, 14, 12, 10 and 8 ka BP in Fig. 3 to show the temporal pattern change of a parameter. The other example is the sensitivity of each parameter at 7 ka BP to compare patterns at a dedicated time. We further note that deposition of sea-level indicators or similar samples on land areas is not possible in glaciated areas. Hence, we mark these areas in the figures by drawing the extent of the ice at a certain time from model Ice-5G.

Figure 3 clearly shows that areas of highest sensitivity to ice-load history changes are located under the ice. Here, sensitivities of more than 600 m are found at 18 ka BP in North America (Fig. 3a). However, it is unlikely to find samples from that time as the area was covered by ice. We therefore focus on ice-free areas. At 18 ka BP, significant sensitivities mainly appear in northern Russia. This is clearly related to differences in the ice models. We therefore draw the ice extent according to model Ice-4G with a green line to allow a rigorous analysis. The extent of the Barents and Kara seas ice sheet in Ice-4G at 18 ka BP is much further to east, and thus there is a clear sensitivity signal visible. Another area is found further east in the Chukchi Sea where Ice-4G contains a glaciation. Both these areas thus show sensitivities of more than 200 m. In all other areas the sensitivity is much less than 100 m. This behavior continues through time as long as the ice sheets significantly remain on the continents. At about 12 ka BP (Fig. 3d) we find a prominent retreat east of the Rocky Mountains uncovering high

SED
5, 2419–2448, 2013

sensitivities of up to 400 m due to significant differences in ice thickness west of Hudson Bay between the two ice models used. Sensitivities of 100 m and more still yield at 7 ka BP (Fig. 4a). In Scandinavia, sensitivities are not that large, but can also reach 50 m at 10 ka BP (Fig. 3e). Similar features are found around Antarctica. In all other areas sensitivities are much lower.

Comparing the patterns of the four parameters (Fig. 4), all other parameters have much lower sensitivities than ice-load history. RSL data are mainly sensitive to lithospheric thickness variations in formerly glaciated areas and also around still glaciated ones. Values of about 12 m are reached. Sensitivity to background viscosity is constrained to the Hudson Bay area and the Antarctic coast. Areas of lower sensitivity can be found around the Arctic and in British Columbia. For sensitivity to lateral viscosity variations, RSL data should be checked in North America, Fennoscandia and Barents Sea.

The results above give an overview of the general sensitivity pattern. However, one has to take the error of RSL data and their likely locations into account. As outlined in Sect. 2, we select an error of 2 m in this preliminary investigation. Figures 5–7 show the sensitivity pattern above 2 m error of all four parameters at 8 selected times on the globe. We mark again the ice extent, but do not cover the continents as it may be possible one day to determine heights above sea level in past times far off the sea. It also allows us to better compare the pattern change of a parameter over time. However, we eventually discuss in Sect. 5 potential RSL data only for areas where RSL data can be expected according to current knowledge.

The dominant parameter when assuming an RSL data error of 2 m is ice-load history. Samples dated to 18 ka BP are sensitive to it almost everywhere in the world (Fig. 5a, red lines), with the exception of the southern Indian Ocean. Smaller areas of lower sensitivity are very local and may disappear or shifted when the error is slightly changed. At later times (Fig. 5b and c), RSL data from all over the world have enough sensitivity to ice-load history. At 12 ka BP (Fig. 5c), the pattern changes more significantly showing low sensitivities in the circum-antarctic oceans. This white space is shifted

2000 yr later to north of the equator with a low-sensitivity region around some part of the Mediterranean and the Black Sea. Thereafter, the whole white space is expanding until 2 ka BP (Fig. 7b) pushing back areas of higher sensitivity to the (former) glaciated regions and leaving local sensitivity areas above 2 m error at certain times. The latter can be found, for example, at 7 ka BP in South America, southern Africa and Australia (Fig. 6c). On the other hand, we note that most coastal areas far away from the former glaciation are insensitive. This holds, for example, since 10 ka BP for a major part of the Mediterranean and some parts of the Caribbean.

The size of areas sensitive to lithospheric thickness variations is much smaller when compared to the ones sensitive to ice-load history. At 18 ka BP (Fig. 5a, green lines), such areas are found near the ice sheets. There are a few spots in the Mediterranean, Central America and in Southeast Asia, however, they are too distinct and can be easily vanish if the error limit or the model is changed. The behavior of the pattern remains throughout all times. Any sensitive area is found near ice sheets or formerly glaciated areas. The distinct spots in mid-latitudes fade out at about 10 ka BP (Fig. 8b). At 2 ka BP (Fig. 7b), only RSL data from the Antarctic Peninsula, the northern Gulf of Bothnia and the Baffin Bay may help in investigations to lithospheric thickness variations.

Sensitivity to background viscosity covers larger areas than sensitivity to lithospheric thickness variations. Almost all area north of 45° N, South America, parts of Africa, East Asia, Australia and Antarctica show a sensitivity above 2 m at 18 ka BP (Fig. 5a, blue dots). This pattern does not change significantly until 12 ka BP (Fig. 5c). Thereafter, the behavior is similar to lithospheric thickness variations as high sensitivity areas are found in the surrounding of the (formerly) glaciated area, although they cover larger areas. At 2 ka BP (Fig. 7b), only a few spots are left on the Northern Hemisphere, with southern James Bay, northern Gulf of Bothnia and the Barents Sea as areas with highest likelihood to find RSL data with sensitivity to background viscosity.

Lateral variations in viscosity show the most diverse sensitivity pattern of the four tested parameters. From 18 ka BP (Fig. 5a, purple lines) until 14 ka BP (Fig. 5b), many areas of sufficient sensitivity are determined next to the immediate surrounding of the ice sheets. Of interest are here the west and northeast coast of South America, the northwest coast of Africa and Australia. In the following millennia the areas are more constrained to the near surrounding of the (formerly) glaciated areas. At 2 ka BP (Fig. 7b), there are only a few very small areas on land in North America left. In Fennoscandia, RSL data from the Lofoten may be helpful.

So far, we have only analysed the sensitivity assuming an RSL data error of 2 m. But, how does the pattern at a specific time change if a different error is assumed? Figure 8 shows the effect of error size (1 m for (a), 2 m for (b) and 8 m for (c)) on the pattern for 10 ka BP. The latter represents a rather extreme case, while an error of 1 m is a likely improvement for more recently discovered and dated samples.

It is clear that any pattern at a specific time will not change significantly if the error value is changed moderately, e.g. by a few decimeters. If the value is changed significantly to higher or lower values, the pattern of a parameter will decrease or increase its sensitivity area accordingly. To understand why the area increases when the error value decreases, note that the plotted areas have sensitivity values (e.g. Figs. 3 and 4) above the error value. Thus a smaller error value means more area can be sensitive to that parameter variation. For example, when the error changes from 2 to 1 m, the global sensitivity pattern of ice-load history shows mainly the same signature as for an error of 2 m, but the area becomes larger reducing the insensitive areas in the Caribbean and the Mediterranean. For all other parameters the pattern increase more drastically around the equator.

As expected, when raising the error to 8 m, the sensitivity area for all parameter is reduced significantly. Sensitivities to lateral variation in viscosity, background viscosity and variation in lithospheric thickness are now mainly found near the glaciated areas. Sufficient information on background viscosity cannot be extracted from RSL data in this case as areas sensitive to it are quite small and restricted. Ice-load history covers larger areas with a majority on the Southern Hemisphere.

SED
5, 2419–2448, 2013

5 Discussion

The results show a high sensitivity of RSL data to ice-load history changes. It is thus confirmed that RSL data play an outstanding important role in the development of such models, especially on a global scale. Over all millennia and almost independent of the chosen error, it is the dominant sensitivity pattern. This is clear due to the link of RSL data indicating sea-level changes to ice coverage via the sea-level equation (Farrell and Clark, 1976). The higher the amount of ocean water bound in ice sheets at a certain time, the larger the sensitivity areas. Meanwhile well-known sea-level fingerprints from the ice sheets (e.g. Mitrovica et al., 2001) also appear in the sensitivity pattern of the RSL data. Hence, we confirm a link of selected, but not all RSL data to a certain ice sheet (Peltier, 2004; Horton et al., 2009).

In view of ice-load history changes and our chosen error limit of 2 m, areas of interest are the east coast of the United States, the southern coasts of South America, Africa and Australia as well as the coast of Antarctica. For the Southern Hemisphere this holds mainly until about 7 ka BP, and RSL data from these areas probably help in constraining the Antarctic Ice Sheet history. Data from the US east coast should help in constraining the Laurentide Ice Sheet, which confirms Horton et al. (2009). From about 8 ka BP on, data from the Hudson Bay will be of additional help. Such data have been collected, for example, by Simon et al. (2011) and shown that ice thickness in the area as included in the Ice-5G model should be reduced by about a forth. We also note a corridor between the Rocky Mountains and Hudson Bay from about 12 ka BP on, where lake-level data of former and still existing lakes may be found. In Fennoscandia both the North and Baltic seas highlight sufficient sensitivities from 12 ka BP on.

RSL data with a maximum error of 2 m that are sensitive to lithospheric thickness can only be found near the ice sheets, and thus may only help in quantifying variations there. Hence, sites far away from any ice sheets (e.g. Africa) will not provide insight to lateral lithospheric variations after about 12 ka BP. However, we also note that this sen-

SED
5, 2419–2448, 2013

sitivity pattern is almost completely covered by the ice-load history sensitivity pattern, thus further evaluation is needed to see if these contributions can be distinguished.

Sensitivity to background viscosity changes, still in view of an error limit of 2 m, is highlighted along all coasts during times of high glaciation, i.e. until 14 ka BP. Thereafter, it is constrained to the formerly glaciated areas, but still overlapped by the ice-load history sensitivity pattern. As background viscosity controls the amount of lithospheric depression due to the ice load and thus influences vertical movements and ocean geometry, the pattern at glacial maximum is clearly characterized by mixture of high sensitivities around and in the glaciated areas as well as high sensitivities in the continents. Thus, older far field RSL data may help determine background viscosity if the ice thickness is known satisfactorily.

Lateral variations in mantle viscosity show an unevenly distributed pattern for 2 m error limit that in older times covers the globe, while from about 10 ka BP on, sensitivity is highest in the (formerly) glaciated areas. The pattern in older times is clearly affected by the model used to describe the lateral variations and thus has to be treated with caution. It is generally similar to the sensitivity of lithospheric thickness variations and background-viscosity changes. Hence, the overlap with ice-load history sensitivity is apparent in most regions and must be taken into account when analyzing RSL data to lateral viscosity variations.

The chosen error of 2 m needs to be compared to the deformation and/or sea-level change at a certain time in an area of interest. We note that the sensitivity exceeds 2 m during glaciation almost everywhere including where RSL data can be expected. After glaciation the sensitivity area becomes smaller as the (calculated) deformation or sea-level change can be less than the chosen error of 2 m. However, more recent RSL data and especially those determined in the last two decades usually have errors smaller than 2 m. In such a case the sensitivity pattern for each parameter will be larger than those shown in Figs. 5–7. Thus, samples from other areas can be used in case their error is smaller than the new limit. In our example at 10 ka BP, using 1 m error limit (Fig. 8), one can clearly see that the pattern for ice-load history shows the smallest variation as the sensitivity in sea level at a specific time between the two tested ice models reaches several hundreds of meters, see Fig. 3. In comparison to that, the other three parameters have smaller sensitivities (Fig. 4), and thus a small change in the error limit can lead to significant changes in the pattern. We thus note that the general findings of our study will not be affected if a moderately different error (e.g. a difference of a few decimeters) than 2 m would be chosen. The difference can be larger though when investigating ice-load history. An increase of the error limit by a factor of 4 (from 2 to 8 m) still highlights the typical sensitivity pattern of ice-load hisory, but with reductions in the equatorial area. In turn, it becomes clear that the other three parameters need accurate RSL data for their determination.

The dominant sensitivity signal of ice-load history supports the findings of Wu et al. (2010) to GPS measurements and Steffen et al. (2012) to gravity observations. As RSL data illustrate vertical deformation, the pattern shape of all sensitivities in Fennoscandia and North America has strong similarities with the sensitivity pattern of the vertical component from GPS and gravity measurements. This holds especially for 4 and 2 ka BP, the times closest to today and thus the time of GPS and gravity measurements. However, the latter measurements are performed on land and thus RSL data provide additional information. Therefore, a combined solution from many different GIA observations is recommended in GIA investigations.

6 Conclusions

We have analyzed the sensitivity of RSL data to four parameters which are important in GIA modelling: ice-load history, lateral lithospheric thickness variations, background viscosity, and lateral lithospheric thickness variations. We provide global sensitivity patterns from the time of the last glacial maximum until 2 ka BP. The pattern maps do not exclude the deep sea and the continents as we hope that there will be methods in future that can give similar information as RSL data today, but from areas on land and far away from the coasts. We find a dominant global sensitivity to ice-load history,

SED
5, 2419–2448, 2013

which generally overlaps the patterns of the other three parameters. These three parameters are mainly constrained to areas of former glaciation, i.e. North America and Fennoscandia. The patterns generally become smaller in more recent times.

As noted earlier, it is not possible to accurately define areas where helpful RSL data can be found as this also depends on adequate deposition situations in the last 18 ka BP in a dedicated area, and if a sea-level indicator survived from the time of its deposition until today. If we assume that RSL data having a maximum error of 2 m are found in near coastal areas and assuming that adequate conditions for deposition and preservation exist(ed), we suggest the following regions in the world to look for more RSL data:

– The coasts and shelfs of South America, Africa, Asia (especially Southeast Asia) and Australia for RSL data covering 18 ka BP until 7 ka BP.

– The Antarctic coast and shelf for RSL data during all millennia.

– The United States coast and shelves for RSL data from 18 ka BP until 6 ka BP.

– Hudson Bay for RSL data from 8 ka BP until today.

– Canadian coast and shelves for RSL data from 10 ka BP until 4 ka BP.

– The Baltic and North seas for RSL data from about 14 ka BP on.

However, we have to add that RSL data from most areas far away from the former glaciated areas are mainly sensitive to ice-load history changes and thus may only help in ice-model developments. We also note again that the distinct patterns at a certain time as shown in this study depend on the background models used and the chosen error limit of 2 m. Therefore, one has to be cautious in interpreting the results as they are not definitive both in time and space. The chosen error limit can be changed within a few decimeters to give similar results, which especially holds for sensitivity to ice-load history. A larger change, however, alters the patterns partly significantly. But, we think that our results are indicative enough as independent studies outlined the importance of many of the regions listed above for detailed GIA investigations and ice-model developments (see e.g. Horton et al., 2009; Lambeck et al., 2012).

In view of improvements in the data error, e.g. when reducing the error from 2 m to 1 m, it is interesting to see that more locations, even outside the near field of GIA, can be used to infer parameters such as background viscosity and lateral heterogeneity.

Due to the dominant overlapping signal of ice-load history, one has to distinguish between regions sensitive to one, two three or all four parameters. Assuming that ice-load history is thoroughly investigated and determined in the future, RSL data sensitive to ice-load history and only one of the other three may help to constrain this particular parameter. The results will improve GIA modelling significantly and may also help in initiatives such as PALSEA (Siddall and Milne, 2012), i.e. may guide interested researcher to check locations of potential RSL data helpful in GIA studies.

In turn, more than 14 000 RSL data samples have been determined in the last decades around the world. However, not all are easily accessible for everyone, thus we cannot clearly evaluate if this database is sufficient and present a definite recommendation for new data to be looked for. Of course, more data are always better, needed and well appreciated! But, one has to thoroughly investigate if new data improve our understanding of the GIA and the Earth's interior. Wu et al. (2013), for example, noted that sensitivity of RSL data to lower-mantle viscosity is constrained to formerly glaciated areas. Our results indicate now that this argument is valid for RSL data from about 6 ka BP until today, but not the case for much older RSL data. Thus, adding hundreds of newly determined far-field data that are dated to 6 ka BP and younger may introduce error to such an investigation.

In view of our investigation, new RSL data should be searched around the world. It is clear that the focus has always been set on coastal areas. However, our sensitivity maps show that the deep sea and many areas on land with lakes have high sensitivities and any sea-level indicator found there can be of help.

A comparison to sensitivity studies with data from geodetic measurements (Wu et al., 2010; Steffen et al., 2012) clearly shows the advantage of RSL data to cover both spatial and temporal effects of GIA. However, it also becomes evident that for a detailed and sufficient analysis of the four parameters, it is inevitable to include all different available data sets in a study as long as their measurement errors allow such an analysis.

Acknowledgements. The Finite-Element calculation was performed with the ABAQUS package from Simulia. This research is supported by an Operating Grant from NSERC of Canada to Patrick Wu and Hansheng Wang is supported by National Natural Science Foundation of China (Grant No. 40825012, 41021003, 41174016, 41274026 and 41204013), National Key Basic Research Program of China (973 Program, grant No. 2012CB957703) and CAS/SAFEA International Partnership Program for Creative Research Teams (KZZD-EW-TZ-05). The figures in this paper are drawn using the GMT graphics package (Wessel and Smith, 1998).

References

Engelhart, S. E., Peltier, W. R., and Horton, B. P.: Holocene relative sea-level changes and glacial isostatic adjustment of the US Atlantic coast, Geology, 39, 751–754, doi:10.1130/G31857.1, 2011. 2422

Farrell, W. E. and Clark, J. A.: On postglacial sea level, Geophys. J. Roy. Astr. S., 46, 647–667, doi:10.1111/j.1365-246X.1976.tb01252.x, 1976. 2432

Horton, B. P., Peltier, W. R., Culver, S. J., Drummond, R., Engelhart, S. E., Kemp, A. C., Mallinson, D., Thieler, E. R., Riggs, S. R., Ames, D. V., and Thomson, K. H.: Holocene sea-level changes along the North Carolina Coastline and their implications for glacial isostatic adjustment models, Quaternary Sci. Rev., 28, 1725–1736, doi:10.1016/j.quascirev.2009.02.002, 2009. 2422, 2432, 2436

Klemann, V. and Wolf, D.: A global data base for late-glacial and Holocene sea-level indicators, Poster presented at WCRP Workshop "Understanding Sea-Level Rise and Variability", Paris, 6–9 June 2006. 2425

Lambeck, K., Smither, C., and Ekman, M.: Tests of glacial rebound models for Fennoscandia based on instrumented sea- and lake-level records, Geophys. J. Int., 135, 375–387, doi:10.1046/j.1365-246X.1998.00643.x, 1998a. 2423

Lambeck, K., Smither, C., and Johnston, P.: Sea-level change, glacial rebound and mantle viscosity for northern Europe, Geophys. J. Int., 134, 102–144, doi:10.1046/j.1365-246x.1998.00541.x, 1998b. 2425, 2427

Lambeck, K., Purcell, A., Zhao, J., and Svensson, N.-O.: The Scandinavian Ice Sheet: from MIS 4 to the end of the Last Glacial Maximum, Boreas, 39, 410–435, doi:10.1111/j.1502-3885.2010.00140.x, 2010. 2425

Lambeck, K., Purcell, A., and Dutton, A.: The anatomy of interglacial sea level: the relationship between sea levels and ice volumes during the Last Interglacial, Earth Planet. Sci. Lett., 4, 315–316, doi:10.1016/j.epsl.2011.08.026, 2012. 2436

Lidberg, M., Johansson, J. M., Scherneck, H.-G., and Milne, G. A.: Recent results based on continuous GPS observations of the GIA process in Fennoscandia from BIFROST, J. Geodyn., 50, 8–18, doi:10.1016/j.jog.2009.11.010, 2010.

Mitrovica, J. X., Tamisiea, M. E., Davis, J. L., and Milne, G. A.: Recent mass balance of polar ice sheets inferred from patterns of global sea-level change, Nature, 409, 1026–1029, doi:10.1038/35059054, 2001. 2432

Pedoja, K., Husson, L., Regard, V., Cobbold, P. R., Ostanciaux, E., Johnson, M. E., Kershaw, S., Saillard, M., Martinod, J., Furgerot, L., Weill, P., and Delcaillau, B.: Relative sea-level fall since the last interglacial stage: are coasts uplifting worldwide?, Earth Sci. Rev., 108, 1–15, doi:10.1016/j.earscirev.2011.05.002, 2011. 2423

Peltier, W. R.: Ice age paleotopography, Science, 265, 195–201, doi:10.1126/science.265.5169.195, 1994. 2427, 2443

Peltier, W. R.: Global glacial isostasy and the surface of the iceage earth: the Ice-5G (VM2) model and GRACE, Annu. Rev. Earth Planet. Sci., 32, 111–149, doi:10.1146/annurev.earth.32.082503.144359, 2004. 2422, 2427, 2432, 2443, 2444, 2445

Siddall, M. and Milne, G. A.: Understanding sea-level change is impossible without both insights from paleo studies and working across disciplines, Earth Planet. Sci. Lett., 2–3, 315–316, doi:10.1016/j.epsl.2011.10.023, 2012. 2436

Simon, K. M., James, T. S., Dyke, A., and Forbes, D. L.: Refining glacial isostatic adjustment models in northern Canada: implications for ice sheet history, sea-level change, and land emergence along the west coast of Hudson Bay, AGU Fall Meeting Abstracts, G23B-04, 2011. 2432

Discussion Paper | Discussion Paper | Discussion Paper | Discussion Paper |

Steffen, H. and Kaufmann, G.: Glacial isostatic adjustment of Scandinavia and northwestern Europe and the radial viscosity structure of the Earth's mantle, Geophys. J. Int., 163, 801–812, doi:10.1111/j.1365-246X.2005.02740.x, 2005.

Steffen, H. and Wu, P.: Glacial isostatic adjustment in Fennoscandia – a review of data and modeling, J. Geodyn., 52, 169–204, doi:10.1016/j.jog.2011.03.002, 2011. 2421, 2422, 2424, 2425, 2427

Steffen, H., Wu, P., and Wang, H.: Optimal locations for absolute gravity measurements and sensitivity of GRACE observations for constraining glacial isostatic adjustment on the Northern Hemisphere, Geophys. J. Int., 190, 1483–1494, doi:10.1111/j.1365-246X.2012.05563.x, 2012. 2421, 2422, 2427, 2434, 2437

Törnqvist, T. E. and Hijma, M. P.: Links between early Holocene ice-sheet decay, sea-level rise and abrupt climate change, Nat. Geosci., 5, 601–606, doi:10.1038/ngeo1536, 2012. 2423

van de Plassche, O.: Sea-Level Research: A Manual for the Collection and Evaluation of Data, GeoBooks, Norwich, 1986. 2424

Vink, A., Steffen, H., Reinhardt, L., and Kaufmann, G.: Holocene relative sea-level change, isostatic subsidence and the radial viscosity structure of the mantle of north-western Europe (Belgium, the Netherlands, Germany, southern North Sea), Quaternary Sci. Rev., 26, 3249–3275, doi:10.1016/j.quascirev.2007.07.014, 2007. 2425, 2426

Wang, H. S., Wu, P., and van der Wal, W.: Using postglacial sea level, crustal velocities and gravity-rate-of-change to constrain the influence of thermal effects on mantle lateral heterogeneities, J. Geodyn., 46, 104–117, doi:10.1016/j.jog.2008.03.003, 2008. 2427, 2440

Wessel, P. and Smith, W. H. F.: New, improved version of generic mapping tools released, EOS, 79, p. 579, doi:10.1029/98EO00426, 1998. 2437

Wu, P., Wang, H. S., and Schotman, H.: Postglacial induced surface motions, sea levels and geoid rates on a spherical, self-gravitating laterally heterogeneous earth, J. Geodyn., 39, 127–142, doi:10.1016/j.jog.2004.08.006, 2005. 2427, 2440

Wu, P., Steffen, H., and Wang, H. S.: Optimal locations for GPS measurements in North America and northern Europe for constraining glacial isostatic adjustment, Geophys. J. Int., 181, 653–664, doi:10.1111/j.1365-246X.2010.04545.x, 2010. 2421, 2422, 2427, 2434, 2437

Wu, P., Wang, H., and Steffen, H.: The role of thermal effect on mantle seismic anomalies under Laurentia and Fennoscandia from observations of glacial isostatic adjustment, Geophys. J. Int., 192, 7–17, doi:10.1093/gji/ggs009, 2013. 2421, 2423, 2427, 2436

Table 1. Model parameters for the reference model and other models for sensitivity tests. LT: lithospheric thickness; UM: upper-mantle viscosity (above 670 km depth); LM1: shallow lower-mantle viscosity (670–1171 km depth); LM2: deep lower-mantle viscosity (1171 km to core-mantle-boundary).

Effect of	Ice Model	LT [km]	UM [Pa s]	LM1 [Pa s]	LM2 [Pa s]
Reference Model	Ice-4G	115	6×10^{20}	3×10^{21}	6×10^{21}
Ice model	Ice-5G	115	6×10^{20}	3×10^{21}	6×10^{21}
Lat. heterogeneous lithosphere	Ice-4G	Lat. Het. Lith (Wu et al., 2005)	6×10^{20}	3×10^{21}	6×10^{21}
Background viscosity	Ice-4G	115	7×10^{20}	10^{22}	10^{22}
Lat. heterogeneous viscosity	Ice-4G	115	Lat. Het. Mantle RF3S20 with $\beta = 0.4$ (Wang et al., 2008)		

Discussion Paper | Discussion Paper | Discussion Paper | Discussion Paper |
SED
5, 2419–2448, 2013
Optimal locations of sea-level indicators in GIA investigations

H. Steffen et al.

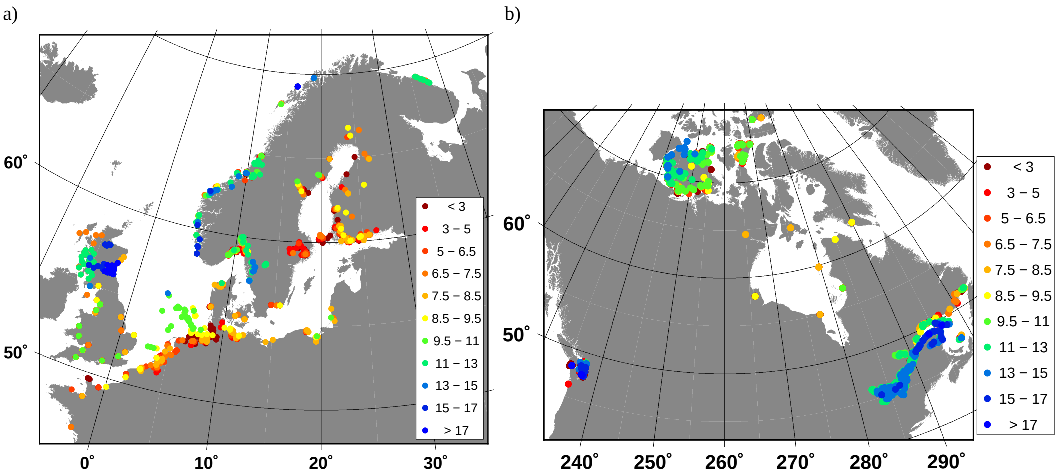

Fig. 1. Exemplary overview of the location of relative sea-level data in **(a)** northern and central Europe, and **(b)** North America. Colored dots highlight their age. Unit in ka BP.

SED
5, 2419–2448, 2013

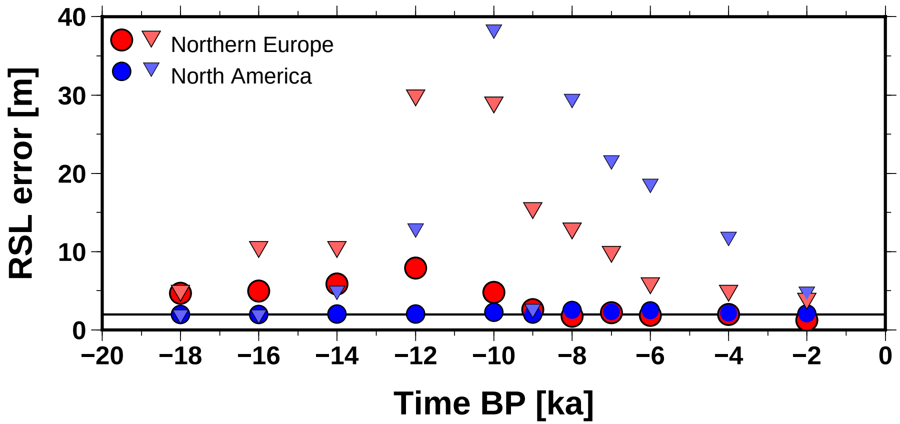

Fig. 2. Average (circles) and maximum (inverted triangles) errors of relative sea-level data in North America (blue) and Europe (red) in time subsets of 1000 (between 10 and 6 ka BP) or 2000 yr. Average calculated as arithmetic mean. In total about 3700 were analyzed for this example.

SED
5, 2419–2448, 2013

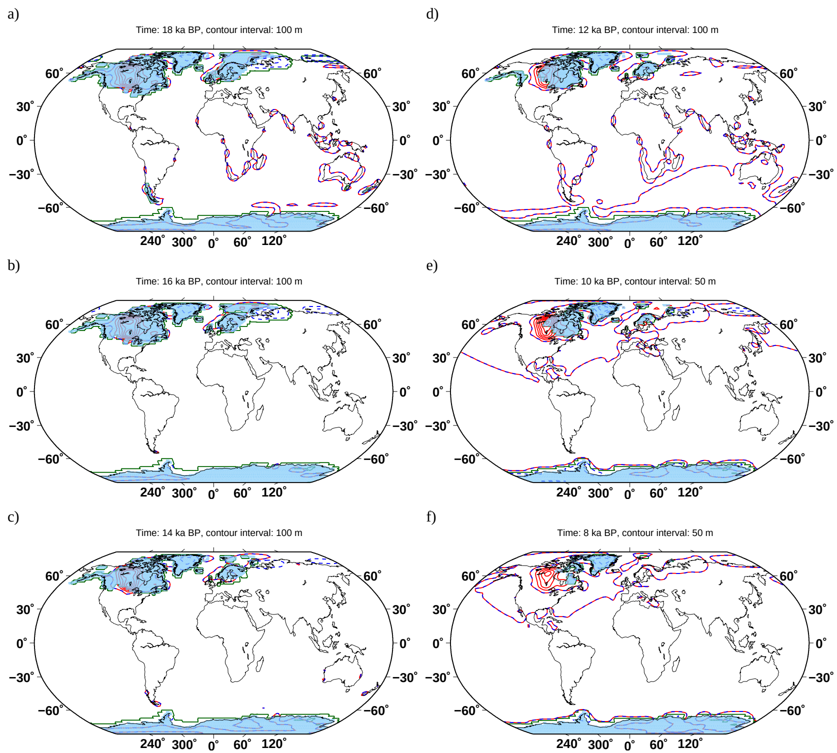

Fig. 3. Sensitivity of relative sea-level data around the world to changes in ice model at **(a)** 18, **(b)** 16, **(c)** 14 ka BP, **(d)** 12, **(e)** 10 and **(c)** 8 ka BP. Light blue areas mark the extent of ice sheets at the time, taken from the Ice-5G model (Peltier, 2004). Green solid line marks the ice extent from the Ice-4G model (Peltier, 1994). Red and blue-dashed lines are contour intervals of positive and negative sensitivity, respectively. The red-blue-dashed line marks zero sensitivity. Intervals indicated on top. Unit in m. To read the sensitivity of a certain line count the number of lines from the zero-sensitivity line and multiply with the interval.

SED
5, 2419–2448, 2013

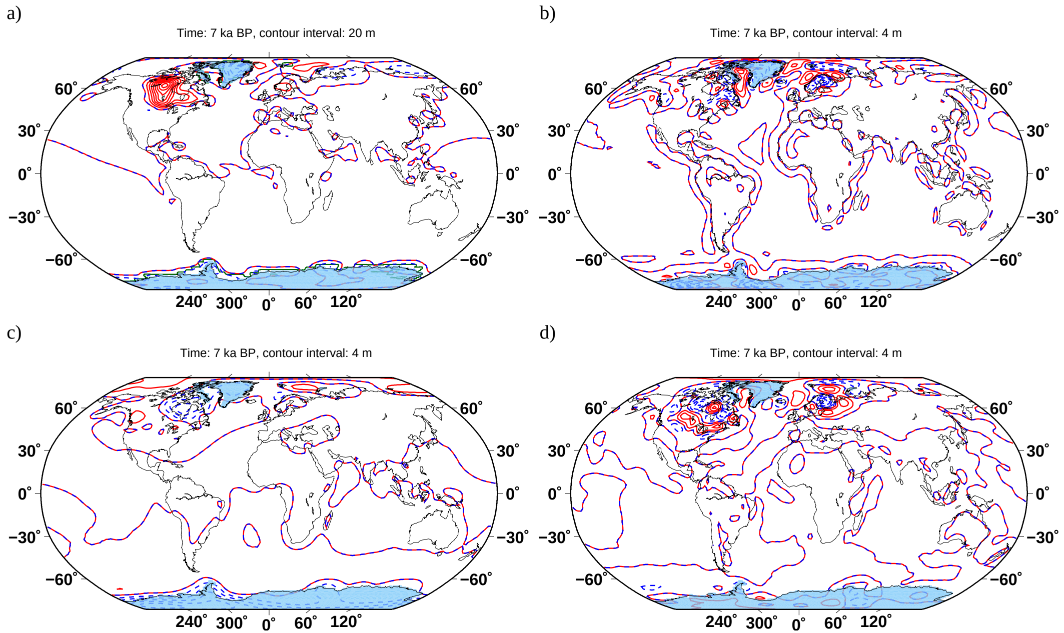

Fig. 4. Sensitivity of relative sea-level data around the world to changes in ice-load history model **(a)**, lithospheric thickness variations **(b)**, background viscosity **(c)**, and lateral viscosity variations **(d)** at 7 ka BP. Light blue areas mark the extent of ice sheets at the time, taken from the Ice-5G model (Peltier, 2004). Red and blue-dashed lines are contour intervals of positive and negative sensitivity, respectively. The red-blue-dashed line marks zero sensitivity. Intervals indicated on top. Unit in m. To read the sensitivity of a certain line count the number of lines from the zero-sensitivity line and multiply with the interval.

SED
5, 2419–2448, 2013

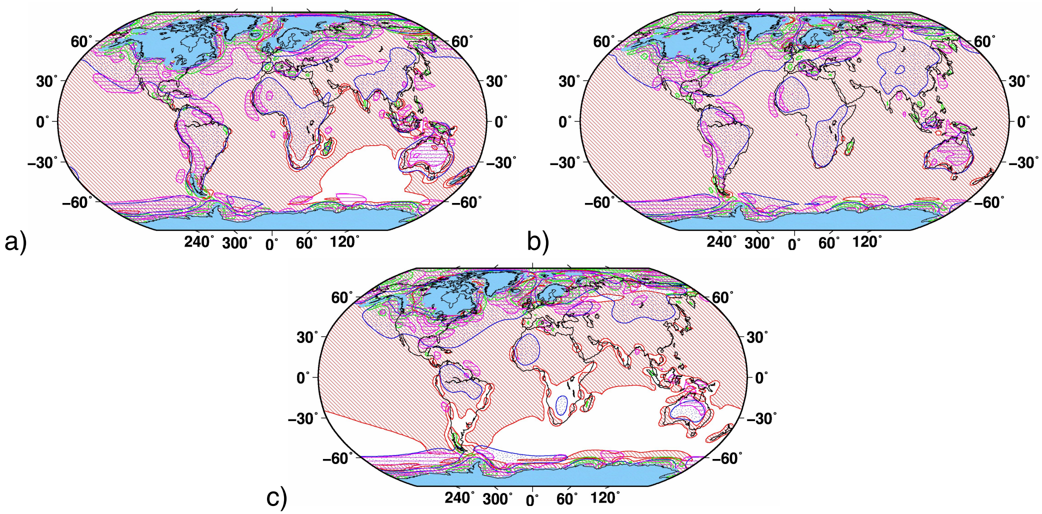

Fig. 5. Sensitivity of relative sea-level data around the world above an assumed error of 2 m to changes in ice-load history model (see text, red area, lines from top left to bottom right), lithospheric thickness variations (green, lines from top right to bottom left), background viscosity (blue dots), and lateral viscosity variations (pink, horizontal lines) at **(a)** 18, **(b)** 14 and **(c)** 12 ka BP. If a color does not appear, then the sensitivity of this parameter lies below the error. Light blue areas mark the extent of ice sheets at the time, taken from the Ice-5G model (Peltier, 2004).

SED
5, 2419–2448, 2013

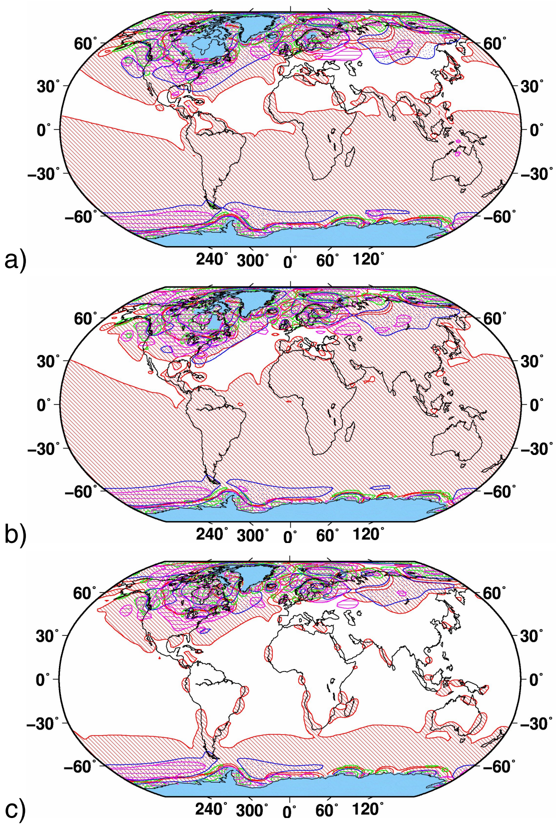

Fig. 6. Same as Fig. 5, but for **(a)** 9, **(b)** 8 and **(c)** 7 ka BP.

SED
5, 2419–2448, 2013

Optimal locations of sea-level indicators in GIA investigations

H. Steffen et al.

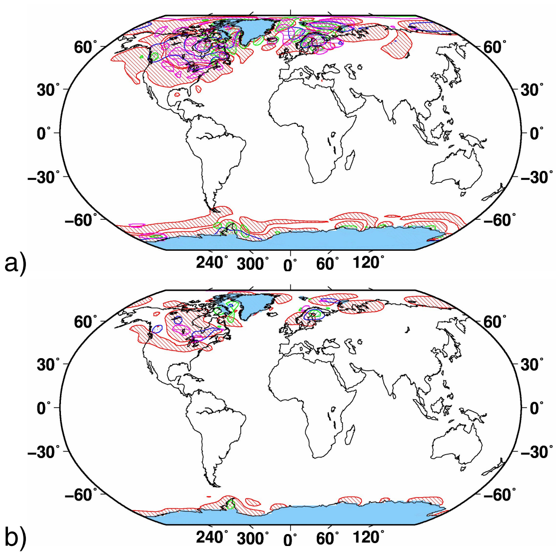

Fig. 7. Same as Fig. 5, but for **(a)** 4, and **(b)** 2 ka BP.

SED
5, 2419–2448, 2013

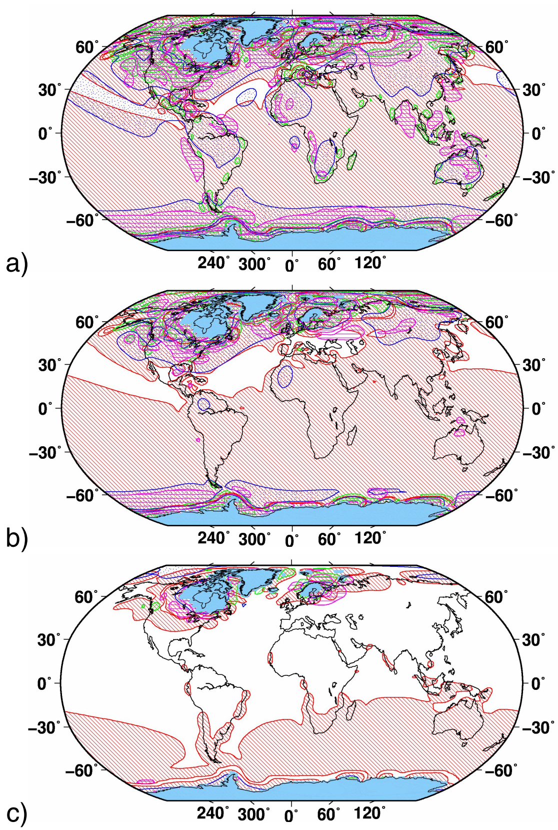

Fig. 8. Same as Fig. 5, but for 10 ka BP and different RSL data errors of **(a)** 1, **(b)** 2 and **(c)** 8 m.

SED
5, 2419–2448, 2013

Optimal locations of sea-level indicators in GIA investigations

H. Steffen et al.